Materials Science & Engineering A 682 (2017) 354–358

Contents lists available at ScienceDirect

Materials Science & Engineering A

journal homepage: www.elsevier.com/locate/msea

Short communication

Room temperature deformation of LPSO structures by non-basal slip

Ran Chen[a,b], Stefanie Sandlöbes[b,c,**], Xiaoqin Zeng[a,*], Dejiang Li[a], Sandra Korte-Kerzel[c], Dierk Raabe[b]

[a] The State Key Laboratory of Metal Matrix Composites, Shanghai Jiao Tong University, 200240 Shanghai, PR China
[b] Max-Planck-Institut für Eisenforschung, Max-Planck-Str. 1, 40237 Düsseldorf, Germany
[c] Institute of Physical Metallurgy and Metal Physics, RWTH Aachen University, 52056 Aachen, Germany

ARTICLE INFO

Keywords:
Mg-LPSO alloy
Deformation mechanisms
Dislocations
Transmission electron microscopy

ABSTRACT

We investigated the deformation mechanisms of long period stacking ordered (LPSO) structures in an extruded $Mg_{97}Y_2Zn_1$ (at%) alloy. Tensile deformation was performed in such a way that basal slip and kink band formation were inhibited. Slip trace analysis and transmission electron microscopy reveal a predominant activity of non-basal <a> slip.

1. Introduction

Magnesium alloys are attractive structural materials due to their low density, high specific strength and good recyclability [1]. However, due to the hexagonal crystal structure of Mg and the related crystallographic anisotropy, only a limited set of slip systems is available resulting in poor room temperature ductility [2,3]. Recently Mg-Y-Zn and Mg-Zn-RE alloys containing long period stacking ordered (LPSO) structures have been reported to possess both high strength and good toughness [4–10]. This excellent mechanical performance has been reported to be related to the presence of LPSO structures, however, the underlying mechanisms for the concomitant increase of strength and toughness are not fully understood [5–11]. LPSO structures are chemically and structurally ordered where RE/Y and Zn atoms occupy Mg positions on neighboring {0001} planes. They share the {0001} basal plane of Mg but are stacking ordered along the c-axis, resulting in stacking periods such as 10H, 14H, 18R and 24R [12–15]. For pure Mg and most magnesium alloys, $\{0001\}\langle 11\bar{2}0\rangle$ basal <a> dislocation slip and $\{10\bar{1}2\}\langle 10\bar{1}\bar{1}\rangle$ twinning are the two predominant deformation mechanisms at room temperature [2,3,16]. However, it has been shown for LPSO structures that twinning is strongly inhibited due to the long stacking periodicity and ordering of RE and Zn atoms [17,18]. Instead, the formation of kink bands has been reported during deformation of LPSO grains, which - together with basal dislocation slip - effectively carries the strain in LPSO structures at room temperature [6–9,11,18–23]. Previous studies also suggest only limited activity of non-basal slip which has been observed only in regions with high local stress concentrations such as adjacent to kink bands during room temperature deformation of LPSO grains [19–22]. Generally, the activation of deformation systems strongly depends on the crystallographic texture and the loading direction [24].

Therefore, this study aims at investigating the active deformation mechanisms in LPSO structures at room temperature under conditions where both, basal slip and kink band formation, are restricted. To this end we investigated the room temperature tensile deformation behavior of an extruded $Mg_{97}Y_2Zn_1$ (at%) alloy which was deformed by tensile loading parallel to the basal planes, hence, restricting the activation of basal slip and kink band formation. By combined slip trace analysis, electron backscatter diffraction (EBSD) and transmission electron microscopy (TEM) we observed a surprising prevalence of non-basal <a> slip in the LPSO structures.

2. Experimental methods

The $Mg_{97}Y_2Zn_1$ (at%) alloy investigated was prepared by electric resistance melting and gravity casting. The ingot was homogenized at 803 K for 30 h and then extruded at 623 K with a reduction rate of 9.97:1 and a ram speed of 2.5 mm s^{-1}. A subsequent heat treatment followed by water quenching was conducted at 773 K for 48 h to release the high strain induced by the extrusion process. After mechanical grinding and polishing, scanning electron microscopy (SEM) and EBSD mapping were applied to examine the microstructure and the crystallographic texture of the longitudinal section of the annealed extrusion bar.

Tensile test samples with gauge dimensions of 4 mm×2 mm×1 mm were prepared along the extrusion direction (ED) by electric discharge

* Corresponding author at: The State Key Laboratory of Metal Matrix Composites, Shanghai Jiao Tong University, 200240 Shanghai, PR China.
** Corresponding author at: Institute of Physical Metallurgy and Metal Physics, RWTH Aachen University, 52056 Aachen, Germany.
E-mail addresses: sandloebes@imm.rwth-aachen.de (S. Sandlöbes), xqzeng@sjtu.edu.cn (X. Zeng).

http://dx.doi.org/10.1016/j.msea.2016.11.056
Received 28 June 2016; Received in revised form 16 November 2016; Accepted 17 November 2016
Available online 18 November 2016
0921-5093/

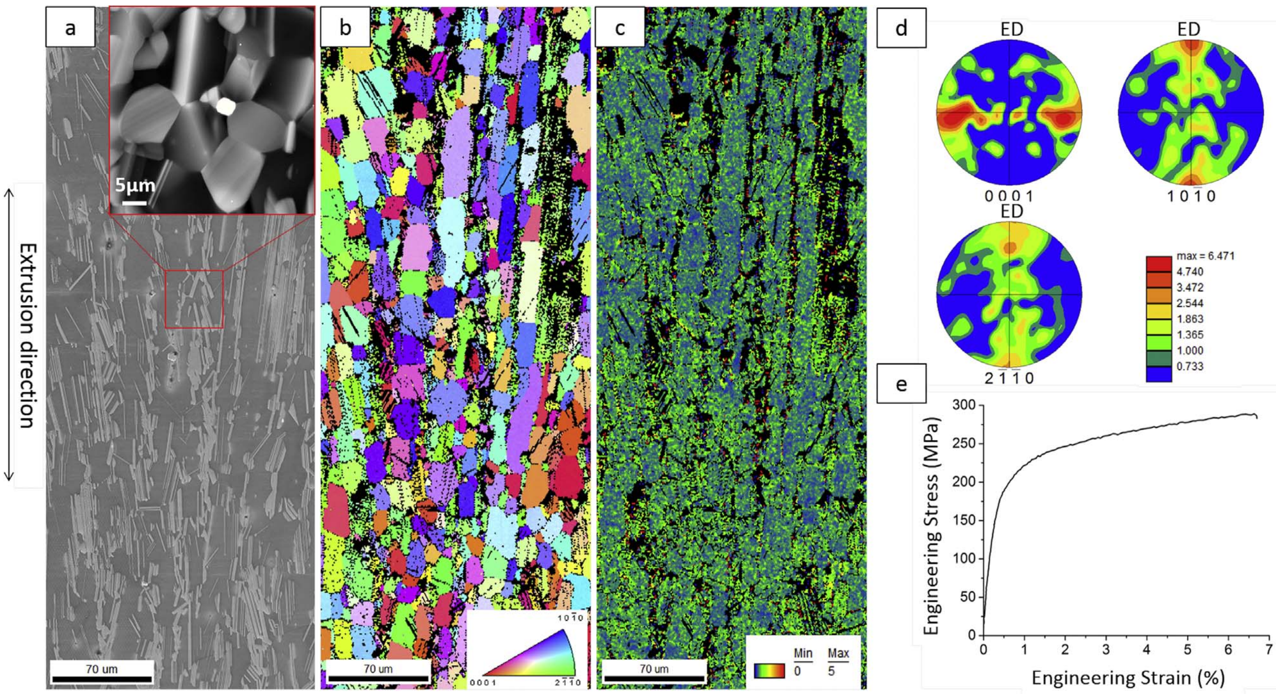

Fig. 1. (a) Secondary electron image, (b) inverse pole figure map of α-Mg and LPSO structure, (c) kernel average misorientation map of α-Mg and LPSO structure, (d) pole figures of the longitudinal sample section representing equally the texture of both microstructural constituents, α-Mg and LPSO structures, due to the $\{0001\}_{LPSO}//\{0001\}_{\alpha\text{-}Mg}$ orientation relationship between α-Mg and LPSO; the inset in (a) shows an enlarged backscattered electron micrograph of the LPSO structures, (e) engineering stress-strain curve of tensile test up to 6.7% strain.

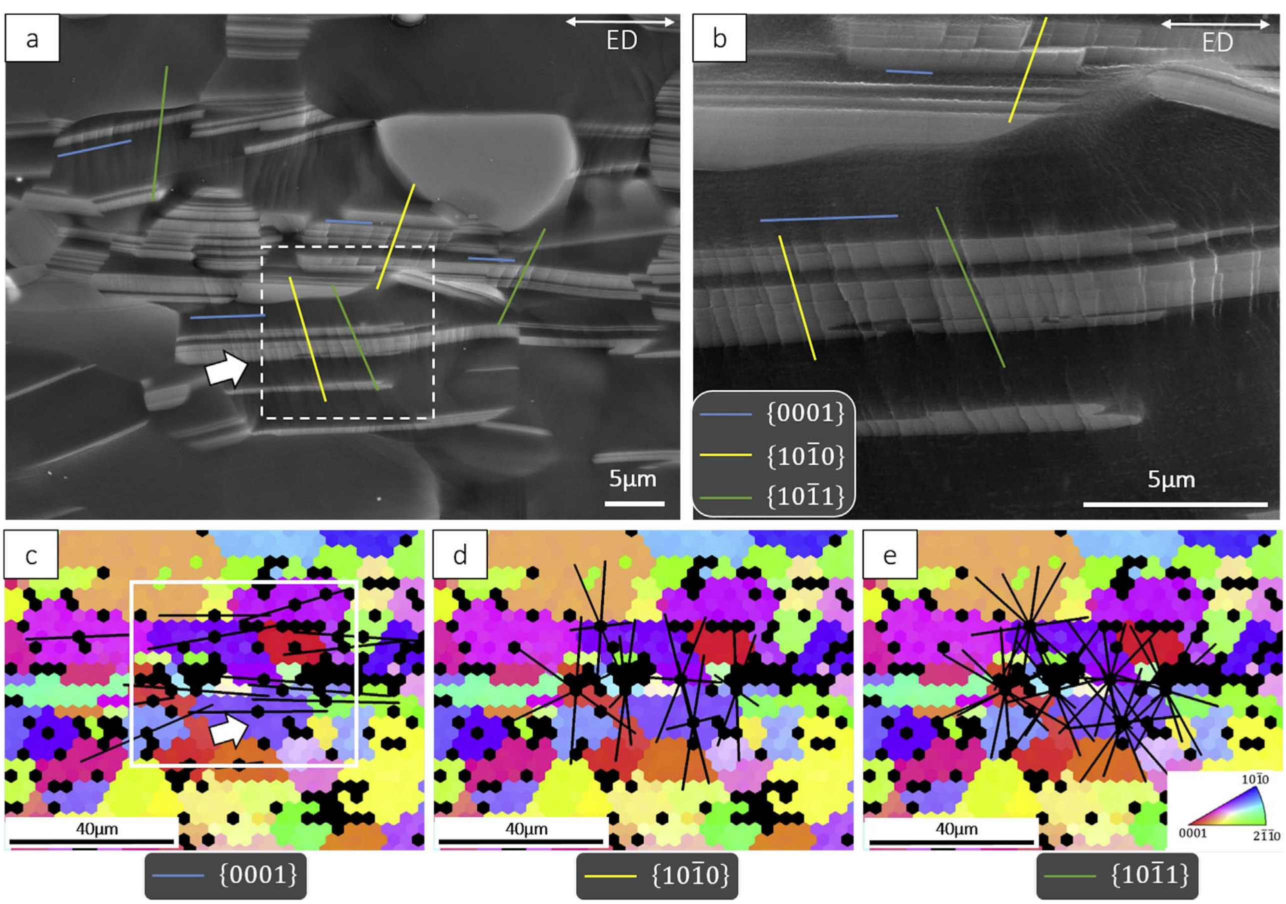

Fig. 2. (a) Secondary electron image of typical slip traces in a sample deformed in tension to 6.7% strain, (b) higher magnification image of the area marked by the rectangle in (a). (c)–(e) Inverse pole figure maps where the $\{0001\}$, $\{10\bar{1}0\}$ and $\{10\bar{1}1\}$ plane traces are marked; the position of the micrograph in (a) is marked by the rectangular in (c).